INT. J. NUM. METH. HEAT FLUID FLOW, VOL. 5, 459–473 (1995)

TRANSIENT CONJUGATED HEAT TRANSFER IN CONCENTRIC ANNULI

M. A. I. EL-SHAARAWI†, M. A. AL-NIMR‡ AND M. A. HADER‡

† *Mechanical Engineering Department, King Fahd University of Petroleum and Minerals, Dhahran 31261, Saudi Arabia*
‡ *Jordan University of Science and Technology, Irbid, Jordan*

ABSTRACT

The paper presents a finite-difference scheme to solve the transient conjugated heat transfer problem in a concentric annulus with simultaneously developing hydrodynamic and thermal boundary layers. The annular forced flow is laminar with constant physical properties. Thermal transient is initiated by a step change in the prescribed isothermal temperature of the inner surface of the inside tube wall while the outer surface of the external tube is kept adiabatic. The effects of solid-fluid conductivity ratio and diffusivity ratio on the thermal behaviour of the flow have been investigated. Numerical results are presented for a fluid of $Pr = 0.7$ flowing in an annulus of radius ratio 0.5 with various values of inner and outer solid wall thicknesses.

KEY WORDS Transient conjugated forced convection Concentric annuli

NOMENCLATURE

C	specific heat capacity
k	thermal conductivity
K_R	thermal conductivity ratio, k_s/k_f
m	number of axial increments in the numerical mesh network
n	number of radial increments inside the fluid in the numerical mesh network
nk	number of time increments in the numerical mesh network
$ns1$	number of radial increments inside the inner tube in the numerical mesh network
$ns2$	number of radial increments inside the outer tube in the numerical mesh network
N_1	inside inner tube radius ratio, r_1/r_3
N_2	outside inner tube ratio, r_2/r_3
N_4	inside outer tube ratio, r_4/r_3
p	pressure
p_0	pressure of the fluid at tube entrance
P	dimensionless pressure, $(p - p_0)/\rho_f u_0^2$
Pr	Prandtl number, ν_f/α_f
Q_{w1}	dimensionless interfacial heat flux at the interface of inner tube and fluid, $q_{w1}/(u\pi\rho C_f(T_w - T_0))$
Q_{w2}	dimensionless interfacial heat flux at interface of outer wall with fluid, $q_{w2}/(u\pi\rho C_f(T_w - T_0))$
r	radial coordinate
r_1	inner radius of inner tube
r_2	outer radius of inner tube
r_3	inner radius of outer tube
r_4	outer radius of outer tube
R	dimensionless radial coordinate, r/r_3
Re	Reynolds number, $\dfrac{2\rho r_3 u_0(1 - N_2)}{\mu_f}$
t	time
T	temperature

0961–5539/95/050459–15$2.00

Received April 1993
Revised March 1994

T_m mixing cup temperature, $\int_{r_1}^{r_2} urT\,dr \Big/ \int_{r_1}^{r_2} ur\,dr$
T_0 fluid temperature at annulus entrance
T_w heated wall temperature
u axial velocity
u_0 average axial velocity
U dimensionless axial velocity, u/u_0
v radial velocity
V dimensionless radial velocity, $\frac{\rho_f v r_3}{\mu_f}$
y coordinate normal to parallel-plate channel walls
Y dimensionless normal coordinate for a parallel-plate channel, y/half channel width
z axial coordinate
Z dimensionless axial coordinate, $\frac{2(1-N_2)z}{r_3 Re}$

Greek symbols

α thermal diffusivity
α_R thermal diffusivity ratio, α_s/α_f
θ dimensionless temperature, $(T-T_0)/(T_w-T_0)$
μ dynamic viscosity
ν kinematic viscosity
ρ density
τ dimensionless time, $\nu_f t/r_3^2$

Subscripts

1 inner tube
2 outer tube
0 inlet or initial conditions
f fluid properties
R ratio
s solid properties
w wall conditions
max maximum

INTRODUCTION

Design calculations and performance parameters of heat exchangers are usually based on the steady state heat transfer values. Transient heat transfer values are however required during periods of start-up, shut-down, and off-normal surges in steady normal operations. Besides, investigations on unsteady forced convection heat transfer in channels are stimulated by the need to procure precise thermal control of heat exchange systems.

In conventional heat transfer analysis, it is common practice to prescribe the temperature or the heat flux at the fluid-wall interface. Consequently, the energy equation for the fluid alone has to be solved in such analyses. The results thus obtained are only good for heat transfer in flows bounded by walls having extremely small thermal resistance besides, in transient cases, infinitely large thermal diffusivity.

However, in actual practice, the wall thermal resistance and diffusivity are finite and hence the thermal conditions at the fluid-wall interface are different from their counterparts imposed at the other surface of the solid wall. Accordingly, the thermal conditions at the fluid-wall interface, which are not known a priori, depend on the thermal properties and flow characteristics of the fluid as well as the dimensions and properties of the solid wall, and can only be obtained by simultaneously solving the energy equations for the fluid and solid media. Such types of problems, where heat conduction in the solid interacts with convective heat transfer, is often referred to as conjugate problems.

Literature until 1976, pertinent to conjugate heat transfer in ducts of various geometrical shapes, has been reviewed by Shah and London[1]. Mori *et al.*[2–4] considered the problem of steady conjugate heat transfer with fully developed laminar flow between parallel plates when there is internal heat generation in the fluid. Using finite-differences, Faghri and Sparrow[5] solved numerically the steady conjugate heat transfer with hydrodynamically fully developed laminar flow in a thick-walled circular tube. The pipe was supposed to extend indefinitely in the axial direction, a portion of its length was uniformly heated, and axial conduction was considered in both the fluid and the wall. Barozzi and Pagliarini[6] used a finite-element method to deal with

the same steady conjugate problem in a pipe of a finite length and axial conduction was considered in the solid only. Pagliarini[7] considered the same problem with the exception that the flow is hydrodynamically developing. Sakakibara *et al.*[8] analytically investigated the steady conjugate heat transfer problem in an annulus with a heated core and an insulated outside tube when the laminar flow is hydrodynamically fully developed.

Using Laplace transform techniques, Kirshan[9] analytically solved the transient conjugate problem for hydrodynamically and thermally fully developed laminar pipe flow with viscous dissipation. He obtained solutions valid for only small values of time after the outer periphery of the pipe undergoes a step change in heat flux or surface temperature. Recently, Olek *et al.*[10] considered the same problem by means of a method of separation of variables and concluded that the degree of conjugation and viscous dissipation may have a great impact on the temperature distribution in the fluid. For periodic variation of the inlet temperature, Cotta *et al.*[11] presented analytical solutions for the problem with slug flow in parallel-plate and circular channels. Lin and Kuo[12] used an implicit finite-difference scheme to obtain numerical solutions for the conjugate unsteady heat transfer to a hydrodynamically fully developed laminar flow (with a Poiseuille velocity profile) in a long circular pipe with a step change in its uniform wall heat flux over a finite length of the pipe wall. They considered axial conduction in both the fluid and the solid and investigated the influences of Peclet number, radius ratio, conductivity ratio and diffusivity ratio on the transient heat transfer characteristics. Neglecting axial conduction in both the fluid and the solid, Yan *et al.*[13] considered the same problem but with a step change in the pipe-wall temperature.

A thorough survey of the literature failed to disclose any prior investigation on the problem of unsteady conjugate (coupled conduction and convection) heat transfer in annular channels. This is in spite of the many applications which employ the annular geometry, e.g. in coolant channels of fuel elements of some nuclear reactors, in double pipe heat exchangers, etc. However, of practical importance to the case under consideration is the conventional problem of steady (with respect to time) flow in the entrance region of concentric annuli with simultaneously developing hydrodynamic and thermal boundary layers. At considerably large values of solid-fluid thermal diffusivity ratio and thermal conductivity ratio, besides extremely thin solid walls, the solution to the transient conjugate problem should asymptotically approach the steady-conventional solution. Hence the latter can provide a limiting case to assess the validity of the proposed finite-difference scheme for the transient conjugate problem and the associated computer program. Such conventional steady solutions were reported by El-Shaarawi[14], Coney and El-Shaarawi[15] and El-Shaarawi and Sarhan[16].

The lack of either theoretical or experimental data concerning the problem of transient conjugate heat transfer in annular passages, and the aforesaid practical importance of this problem, motivated the present work. The present paper is concerned with transient conjugate heat transfer to a laminar forced flow with constant physical properties in the entry region of a concentric annulus. Heating starts at the entrance cross-section and thus the hydrodynamic and thermal boundary layers are developing, with respect to the space coordinates (r and z), simultaneously. However, the velocity profiles are taken to be stationary (steady) with respect to time. Thermal transient is caused by a step change in the isothermal temperature of the inner surface of the core tube while the outer surface of the external tube is kept adiabatic. As a consequence of the assumption of constant fluid properties, the hydrodynamic boundary layers and their associated velocity profiles would remain stationary (steady with respect to time) after the thermal transient has been initiated.

GOVERNING EQUATIONS

Figure 1 depicts the geometry and coordinate system used. The fluid enters the annular passage with a uniform velocity distribution, u_0, which is unchanging in time. Prior to the start of the

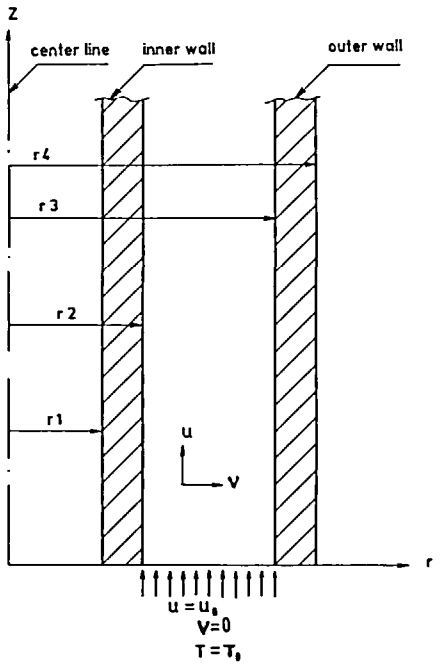

Figure 1 Geometry and coordinate system

step change in the temperature of the inner surface of the core tube, the fluid may either be in a thermal steady-state as a result of some previous steady heat transfer process, or alternately, the fluid and the annulus walls may be at the same uniform temperature, T_0. The transient conjugate heat transfer process starts at $t > 0$.

Assuming axisymmetric, laminar, boundary-layer flow of a Newtonian (linear viscous) fluid, with no internal heat generation in the fluid and its bounding inner and outer solid walls which have the same thermal conductivity (k_s), neglecting viscous dissipation ($2\mu(\partial u/\partial z)^2$) and the axial conduction of heat in the solid walls ($k_s(\partial^2 T/\partial z^2)$) and in the fluid ($k_f(\partial^2 T/\partial z^2)$), and using the dimensionless parameters given in the nomenclature, the equations of continuity, z-momentum, energy for the fluid and energy for the inner or outer solid wall reduce to the following dimensionless equations, respectively:

$$\frac{\partial U}{\partial Z}+\frac{1}{R}\frac{\partial (RV)}{\partial R}=0 \tag{1}$$

$$U\frac{\partial U}{\partial Z}+V\frac{\partial U}{\partial R}=-\frac{\partial P}{\partial Z}+\frac{1}{R}\frac{\partial}{\partial R}\left(R\frac{\partial U}{\partial R}\right) \tag{2}$$

$$\frac{\partial \theta_f}{\partial \tau}+U\frac{\partial \theta_f}{\partial Z}+V\frac{\partial \theta_f}{\partial R}=\frac{1}{Pr}\left[\frac{1}{R}\frac{\partial}{\partial R}\left(R\frac{\partial \theta_f}{\partial R}\right)\right] \tag{3}$$

$$\frac{\partial \theta_s}{\partial \tau}=\frac{\alpha_R}{Pr}\frac{1}{R}\frac{\partial}{\partial R}\left(R\frac{\partial \theta_s}{\partial R}\right) \tag{4}$$

It is worth noting that the radial momentum equation has been eliminated due to the boundary-layer simplifications. However, it is possible[14–16], under the numerical scheme of Bodoia and Osterle[17], to compensate for the lack of such an equation by using the following

dimensionless integral continuity equation:

$$\int_{N_2}^{1} UR\,dR = \frac{1}{2}(1 - N_2^2) \tag{5}$$

Due to the assumption of constant physical properties, the energy (3) for the fluid is not coupled with the equations of conservation of mass and momentum (1 and 2). Thus, the hydrodynamics of the flow in the present work are independent of both temperature and time. Therefore, the equations of conservation of mass and momentum (1 and 2) can be solved to determine the axial and radial velocity profiles (U and V), after which the energy equations (3 and 4) can be solved using the previously obtained velocity profiles. The initial and boundary conditions for the case under consideration are given in dimensionless forms hereunder:

$$\text{for} \quad \tau \leqslant 0,\ Z = 0 \quad \text{and} \quad N_2 \leqslant R \leqslant 1$$
$$U = 1,\ V = 0,\ P = 0 \quad \text{and} \quad \theta_f = 0 \tag{6a}$$
$$\text{for} \quad \tau \leqslant 0,\ Z = 0,\ N_1 \leqslant R \leqslant N_2 \quad \text{and} \quad 1 \leqslant R \leqslant N_4$$
$$\theta_s = 0 \tag{6b}$$
$$\text{for} \quad \tau \leqslant 0,\ Z > 0 \quad \text{and} \quad N_1 \leqslant R \leqslant N_4$$
$$\theta_f = \theta_s = 0 \tag{6c}$$
$$\text{for} \quad \tau > 0,\ Z = 0 \quad \text{and} \quad N_2 < R < 1$$
$$U = 1,\ P = 0,\ V = 0 \quad \text{and} \quad \theta_f = 0 \tag{6d}$$
$$\text{for} \quad \tau > 0,\ Z > 0,\ R = N_2 \quad \text{and} \quad R = 1$$
$$U = 0,\ V = 0,\ \theta_s = \theta_f \quad \text{and} \quad K_R \frac{\partial \theta_s}{\partial R} = \frac{\partial \theta_f}{\partial R} \tag{6e}$$
$$\text{for} \quad \tau > 0,\ Z = 0,\ N_1 \leqslant R \leqslant N_2 \quad \text{and} \quad 1 \leqslant R \leqslant N_4$$
$$\theta_s = 0 \tag{6f}$$
$$\text{for} \quad \tau > 0,\ Z > 0 \quad \text{and} \quad R = N_1$$
$$\theta_s = 1 \tag{6g}$$
$$\text{for} \quad \tau > 0,\ Z > 0 \quad \text{and} \quad R = N_4$$
$$\frac{\partial \theta_s}{\partial R} = 0 \tag{6h}$$

NUMERICAL METHODOLOGY

To convert the governing equations (1)–(4) into finite-difference equations, a 3-dimensional parallelpiped grid in R, Z and τ has to be imposed on half of the channel and (i, j, k) is a typical mesh point; only half of the channel is needed due to symmetry about the Z-axis. The rectangular grid shown in *Figure 2a* is superimposed on half of the channel in the R–Z plane; this grid can be used only once to get the velocity field and it represents the thermal solution domain for $\tau = 0$. For other values of τ, there are identical parallel grids, i.e. the dimensionless time (τ) is simulated as a third coordinate normal to R–Z plane as clarified in *Figure 2b*. The number of radial increments in the inner solid wall, the fluid, and the outer solid wall are *ns*1, *n* and *ns*2, respectively. Mesh points are numbered consecutively: i progresses in the radial direction, with $i = 1$ at the inner surface of the core tube, $i = ns1 + 1$ at the inner fluid-solid interface,

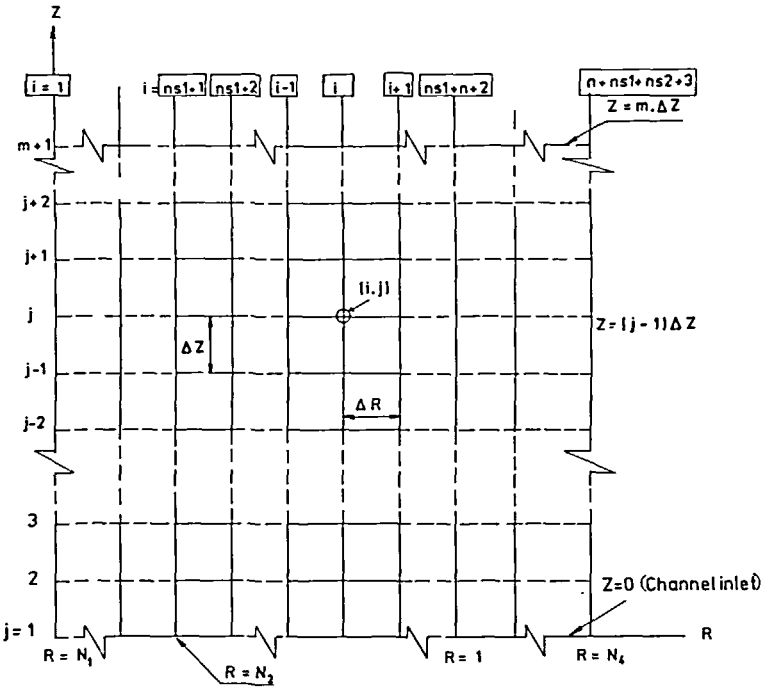

Figure 2 (a) Numerical grid in R–Z plane

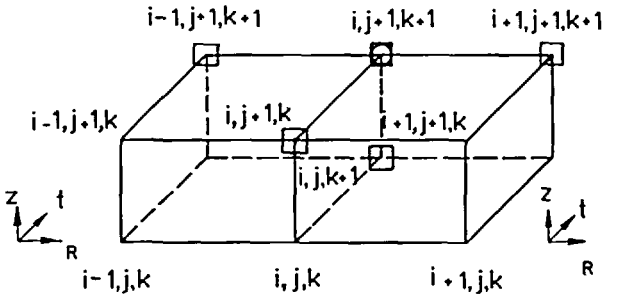

Figure 2 (b) Three dimensional grid for energy equations

$i = ns1 + n + 2$ at the outer fluid-solid interface, and $i = ns1 + n + ns2 + 3$ at the outer surface of the external tube; j progresses in the axial direction, with $j = 1$ at the inlet cross section and $j = m + 1$ at the final cross section; and k progresses in the fictitious time direction, with $k = 1$ at the initial state and $k = nk + 1$ at the final state. The value of m (number of steps in the axial direction) is chosen such that hydrodynamic full development is obtained and the value of nk is chosen such that steady-state conditions are achieved.

Since U and V are independent of τ and θ, the finite-difference equations corresponding to (1) and (2) can be constructed in the R–Z plane with the two dependent variables U and V having only two subscripts (i) and (j). Moreover, since P is a function of Z only, it can have only one subscript (j). On the other hand the three-dimensional grid depicted in *Figure 2b* is applicable to the energy equations (3) and (4) since the temperature is a three-dimensional variable.

The numerical scheme used in this investigation is an extension of the linearized finite-difference scheme reported in References 14–17; it takes the unsteady terms and conduction equations into consideration. Central differences and conventional three-point differences are respectively used to replace the first and second derivatives with respect to R. Backward differences are used to replace the derivatives with respect to τ and Z. Thus the scheme is implicit in τ and Z (doubly-implicit).

With replacement of the derivatives at the points $(i+\frac{1}{2}, j+1)$ and $(i+1, j+1)$ in the continuity and z-momentum equations, respectively, by finite-differences, these two equations can take the following forms, respectively:

$$V_{i+1,j+1} = A_i' V_{i,j+1} - B_i'[U_{i+1,j+1} + U_{i,j+1} - U_{i+1,j} + U_{i,j}] \tag{7}$$

where

$$A_i' = \left[\frac{N_2 + (i-1)\Delta R}{N_2 + i\Delta R}\right]$$

$$B_i' = \frac{\Delta R}{4\Delta Z}\left[\frac{2N_2 + (2i-1)\Delta R}{N_2 + i\Delta R}\right]$$

and

$$A_i U_{i-1,j+1} + B_i U_{i,j+1} + C_i U_{i+1,j+1} + P_{j+1} = D_i \tag{8}$$

where

$$A_i = \frac{\Delta Z}{\Delta R}\left[-\frac{V_{i,j}}{2} + \frac{1}{2[N_2 + (i-1)\Delta R]} - \frac{1}{\Delta R}\right]$$

$$B_i = U_{i,j} + \frac{2\Delta Z}{(\Delta R)^2}$$

$$C_i = \frac{\Delta Z}{\Delta R}\left[\frac{V_{i,j}}{2} - \frac{1}{2[N_2 + (i-1)\Delta R]} - \frac{1}{\Delta R}\right]$$

and

$$D_i = (U_{i,j})^2 + P_j$$

With the replacement of the derivatives at the point $(i, j+1, k+1)$ in (3) and (4) by finite-differences, these two equations can be written as follows, respectively:

$$\dot{A}_i \theta_{i-1,j+1,k+1} + \dot{B}_i \theta_{i,j+1,k+1} + \dot{C}_i \theta_{i+1,j+1,k+1} = \dot{D}_i \tag{9}$$

where

$$\dot{A}_i = \frac{1}{2Pr\Delta R[N_2 + (i-1)\Delta R]} - \frac{1}{Pr(\Delta R)^2} - \frac{V_{i,j}}{2\Delta R}$$

$$\dot{B}_i = \frac{1}{\Delta\tau} + \frac{U_{i,j}}{\Delta Z} + \frac{2}{Pr(\Delta R)^2}$$

$$\dot{C}_i = \frac{V_{i,j}}{2\Delta R} - \frac{1}{Pr(\Delta R)^2} - \frac{1}{2Pr\Delta R[N_2 + (i-1)\Delta R]}$$

and

$$\dot{D}_i = \frac{\theta_{i,j+1,k}}{\Delta\tau} + \frac{U_{i,j}}{\Delta Z}\theta_{i,j,k+1}$$

and

$$\hat{A}_i\theta_{i-1,j+1,k+1} + \hat{B}_i\theta_{i,j+1,k+1} + \hat{C}_i\theta_{i+1,j+1,k+1} = \hat{D}_i \tag{10}$$

where

$$\hat{A}_i = \frac{\alpha_R}{2Pr\Delta R[N_2 + (i-1)\Delta R]} - \frac{\alpha_R}{Pr(\Delta R)^2}$$

$$\hat{B}_i = \frac{1}{\Delta\tau} + \frac{2\alpha_R}{Pr(\Delta R)^2}$$

$$\hat{C}_i = \frac{\alpha_R}{Pr(\Delta R)^2} - \frac{\alpha_R}{2Pr\Delta R[N_2 + (i-1)\Delta R]}$$

$$\hat{D}_i = \frac{\theta_{i,j+1,k}}{\Delta\tau}$$

By means of the trapezoidal rule, (5) becomes:

$$\sum_{i=1}^{n-1} U_{i,j}(N_2 + i\Delta R) = \frac{n(1+N_2)}{2} \tag{11}$$

The numerical solution is obtained by first selecting values of the controlling parameters. The present conjugated heat transfer problem is dependent on six dimensionless parameters, namely, Pr, α_R, K_R, N_1, N_2, and N_4. The first and fifth of these parameters (Pr) and (N_2) are common between the present case and the conventional problem in References 14–16 while the other four parameters are the result of the conjugation process.

The procedure of solving (8) and (11) to get U and P at each cross-section, after which (7) is used for the computation of V at the same cross-section, is discussed in Reference 15. Now, having obtained values of U and V at a cross-section (j), (9) and (10) associated with the conditions (6) can be used to obtain the temperature values at $\tau + \Delta\tau$. In equations (9) and (10) θs with subscript k are known and those with subscript $k+1$ are unknowns.

At a given cross-section, the application of (10) with $i = 2, 3, \ldots, ns1$ (in the inner solid wall) gives ($ns1 - 1$) linear algebraic equations in $ns1$ unknown values of θ. The application of a finite-difference representation of condition (6e) at $i = ns1 + 1$ (i.e., at $R = N_2$) with a backward difference in the solid and a forward difference in the fluid gives an equation linking values of θ at $i = ns1, ns1 + 1, ns1 + 2$. Thus, the number of equations has increased by one but the number of unknowns has also increased by one. Now, (9) is applied with values of i from $ns1 + 2$ until $ns1 + n + 1$ (i.e., in the fluid region) to obtain n additional linear equations. Then, the application of a finite difference representation of condition (6e) at $i = ns1 + n + 2$ (i.e., at the outer fluid-solid interface) gives an equation in values of θ at $i = ns1 + n + 1, ns1 + n + 2$ and $ns1 + n + 3$. Equation (10) is applied at this stage with values of i from $ns1 + n + 3$ until $ns1 + n + ns2 + 1$ to give $ns2 - 1$ additional equations. Finally, a backward difference representation of condition (6h) is applied at $i = ns1 + n + ns2 + 2$ to obtain one more equation.

A summing-up of the aforesaid procedure is as follows: the applications of (9) and (10), the condition (6e) at the two fluid-solid interfaces, and the condition (6h) at the outer boundary, with i varying in a unit step from $i = 2$ to $i = ns1 + n + ns2 + 2$, gives $ns1 + n + ns2 + 1$ linear algebraic equations in the same number of θ-unknowns. By following the previously mentioned sequence, the matrix of coefficients of this set of equations is tridiagonal. Hence the Thomas method[18], which requires low computer storage, can be used to obtain the unknown values of θ after each time step. Repeating this procedure we can advance in the time domain until the steady-state conditions are achieved.

RESULTS AND DISCUSSION

To verify the adequacy of the present numerical solution, three special computer runs were made in the limiting case in which the wall-to-fluid conductivity ratio and diffusivity ratio are very large and the inner and outer wall thicknesses are very small (N_1 and N_4 are very close to N_2 and unity, respectively). The first of these two runs was made with a value of N_2 very close to unity (to approach the parallel-plate channel; $N_2 = 0.99$) and with a step temperature change at both walls. The obtained unsteady temperature profiles are compared with those of Siegel and Sparrow[19] in *Figure 3* for the single value of Z at which Siegel and Sparrow[19] presented their results. As shown in *Figure 3*, the obtained temperature profiles are generally higher than those of Siegel and Sparrow[19]. This is anticipated since Siegel and Sparrow[19] assumed a fully developed flow while in the present work the flow velocity is developing and hence enhancing the convection heat transfer process. However, making a second special computer run, with a fully developed velocity profile right from the annulus entrance, the difference between the obtained results and those of Siegel and Sparrow[19] becomes unremarkable and the temperature profiles obtained are coincident of those of Siegel and Sparrow.

The same conventional parallel-plate channel problem was solved by Cotta and Ozisik[20] and this provides another check. *Table 1* compares the obtained dimensionless wall heat flux with that of Cotta and Ozisik[20]. As can be seen from this table the present results (for $N_2 = 0.99$) are in very good agreement with those of Reference 20 for values of $\tau \leqslant 0.05$; the maximum percentage difference is about 1.2%. However, for large values of τ (namely 0.1) the percentage difference is about 18.5% which is relatively high. Such a large difference (at high values of τ) is due to the fact that for high values of τ ($\tau > Z/U_{max}$) the flow is far from the conduction region in which the presented results of Cotta and Ozisik are valid.

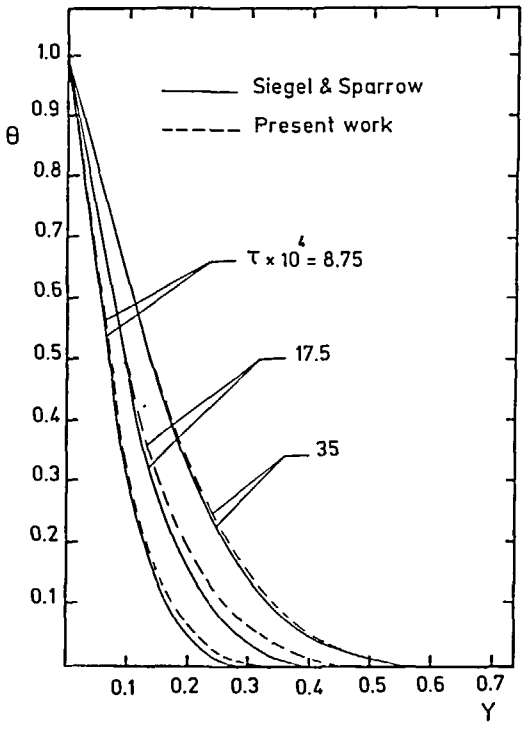

Figure 3 Comparison of the present temperature profiles with those of Siegel and Sparrow[19], $N = 0.99, Z = 2.8 \times 10^{-3}$

Table 1 Comparison of the results of Cotta and Ozisik[20] with those of the present scheme for the conventional problem in a parallel-plate channel

	Q	
τ	Present work	Cotta and Ozisik[20]
0.005	7.970	7.979
0.010	5.660	5.642
0.030	3.275	3.257
0.050	2.250	2.532
0.100	1.505	1.784

The third special computer run was made in the aforesaid limiting case (extremely thin walls of very high thermal conductivity and thermal diffusivity) and the obtained results at considerably large values of τ were found in excellent agreement with the conventional steady-state results which were previously reported in References 1, 14–16. All these comparisons lend support for the adequacy of the present numerical scheme, its associated computer program and the results obtained.

While computations can be conducted for any combination of the controlling dimensionless parameters (Pr, K_R, α_R, N_1, N_2 and N_4), the objective here is to present a sample of results that could illustrate the phenomena pertinent to conjugation and the effect of the consideration of the presence of solid walls on the transient developing forced convection. The computations were carried out for only one value of Prandtl number, namely, 0.7, in a fluid annulus of radius ratio (N_2) = 0.5. The radius ratio 0.5 (for the fluid region) was chosen as it represents a typical annular geometry far enough from the case of parallel-plate channels (for which the radius ratio is unity).

Figures 4a and *4b* give the variation of the radial temperature profiles with time at two selected axial locations, namely $Z = 3 \times 10^{-4}$ and 3×10^{-3}. A careful investigation of these two figures reveals that at very small values of time, e.g. $\tau = 10^{-5}$, the step temperature signal is only felt in the solid wall without reaching the solid-fluid interface and accordingly both the solid region adjacent to the flowing fluid and the fluid remain at the initial temperature. However, as the time elapses the internal solid temperature increases, the temperature signal penetrates in the solid towards the solid-fluid interface, the interface temperature eventually increases above its

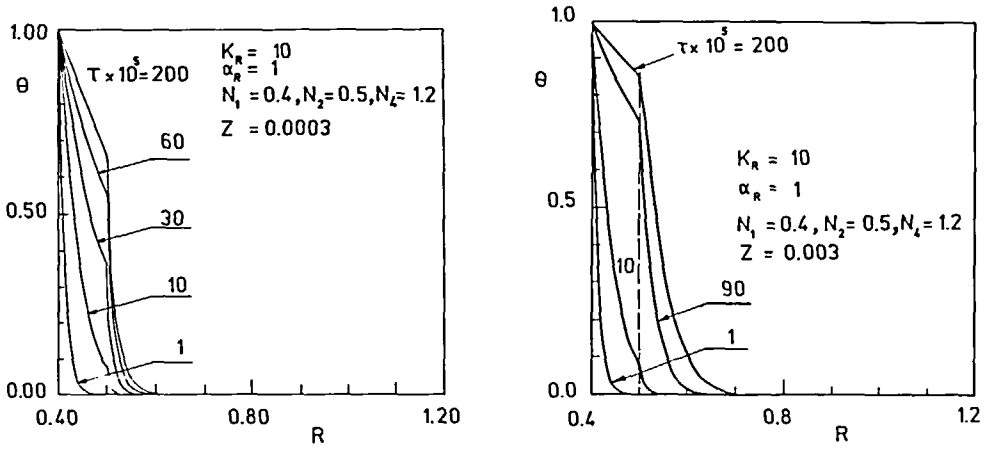

Figure 4 (a) Transient temperature profiles for $Z = 0.0003$ (b) Transient temperature profiles for $Z = 0.003$

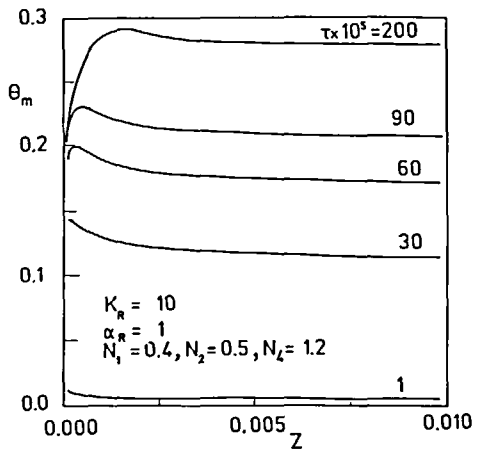

Figure 5 Mixing-cup temperature versus Z for various values of τ

initial value and the fluid starts to feel this temperature signal and warms up. Moreover, at large values of τ (e.g. $\tau = 0.002$ in the Figures) and a given value of R an increase in the value of Z means an increase in the internal temperature of the solid wall, the interfacial solid-fluid temperature, or the fluid temperature. This is attributed to the growth of the hydrodynamic boundary-layer thickness as the fluid moves away from the entrance; the hydrodynamic boundary layer causes a resistance to the heat transfer process.

Thermal and control engineers are not frequently interested in the details of the temperature profiles but only in the fluid mixing-cup (mixed-mean or bulk) temperature and the wall heat flux. The practical importance of θ_m derives from its use in combination with the heat capacity and the inlet temperature of the fluid to determine the heat gained by the fluid without need to get the local and then (by integration) the average heat transfer coefficients. For small values of τ in an annulus having $N_1 = 0.4$, $N_2 = 0.5$, $N_4 = 1.2$, $K_R = 10$ and $\alpha_R = 1$, *Figure 5* presents the dimensionless mixing-cup temperature against the dimensionless axial distance with the time (τ) as a parameter. As can be seen from this figure, for a given τ, the mixing-cup temperature reaches a maximum near the entrance. This phenomenon is explained as follows. At early times, the diffusion term represented by the RHS of (3) is the dominant term for the heat transfer process. In other words, at early times ($\tau < Z/U_{max}$) convection (represented by the terms containing velocity components on the LHS of (3)) is small compared with diffusion and the problem is very much similar to the conduction case. Also, the hydrodynamic boundary layer (which is known to cause the greatest resistance to the radial diffusion of heat) has small thickness near the entrance. Moreover, the radial velocity component V, which is responsible for transporting fluid from regions close to the heated boundary to the core region, has large values near the entrance and decays as the flow moves away from the entrance. Thus, near the entrance and at early times, there is high radial diffusion of heat besides high radial transportation of heat. These two simultaneous effects result in the maximization of the mixing cup temperature near the entrance at early times, as shown in *Figure 5*.

As was explained by Faghri and Sparrow[5] the local Nusselt number in conjugate heat transfer problems includes three unknowns, namely q_{w1}, θ_{w1} and θ_m; hence it is not very informative in such conjugate cases. Instead, the interfacial heat flux distribution is usually presented. The unsteady distribution of the non-dimensional inner wall interfacial heat flux (Q_{w1}) is shown (for the same previously mentioned annulus) in *Figure 6* against the dimensionless time with Z as a parameter. A number of interesting features are unveiled in this figure. Firstly, at early times ($\tau <$ about 0.0002), Q_{w1} grows very quickly and it does not remarkably vary with Z (i.e., it is

rather uniform in the axial direction). This is due to the domination of the radial conduction mode over the forced convection during the initial transient as was previously explained. Secondly, for a given Z the interfacial heat flux reaches a maximum at early times and this maximum occurs at smaller values of τ as Z decreases. Moreover, each curve corresponding to a given Z reaches its steady state value at large values of τ. However, the time required to reach the steady state value increases as the value of Z increases. Again these latter two phenomena can be attributed to the previously mentioned high radial diffusion of heat (due to the thin boundary layer thickness) besides the high radial transportation of heat (due to large values of V) near the entrance (at small values of Z). Thirdly, at a given large value of τ, as the distance from the entrance (Z) increases the wall heat flux decreases. This is due to the increase in the hydrodynamic boundary-layer thickness with Z.

Figures 7, 8 and *9* present, for given values of Z in the previously mentioned annulus, the effect of the wall-to-fluid thermal conductivity ratio (K_R) on the variations with time of the inner

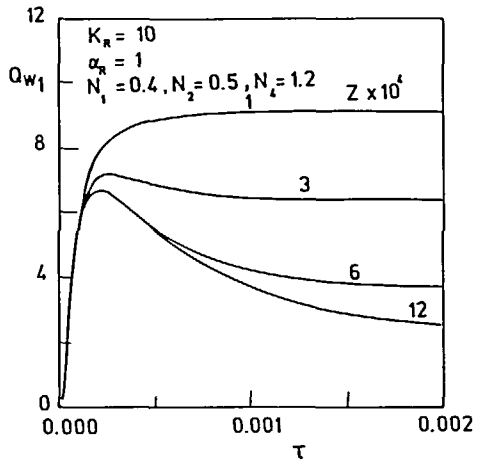

Figure 6 Inner wall heat flux versus τ at various values of Z

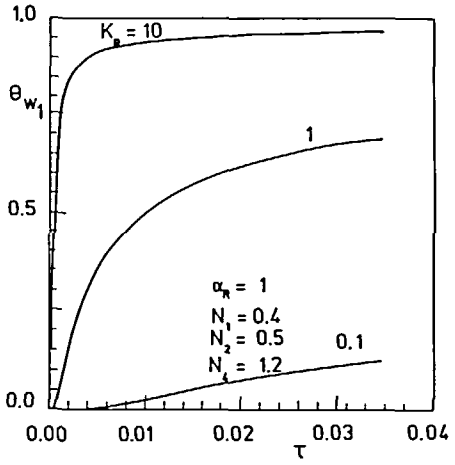

Figure 7 Effect of K_R on the transient behaviour of the inner interfacial temperature, $Z = 3.5 \times 10^{-4}$

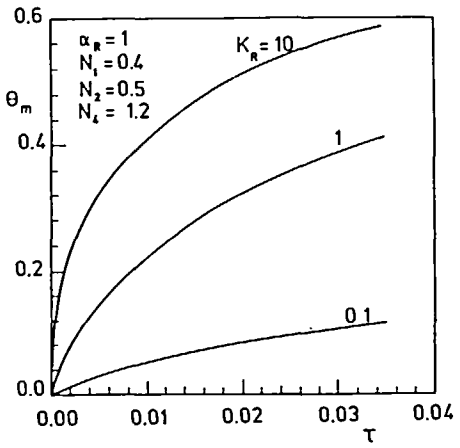

Figure 8 Effect of K_R on the transient behaviour of θ_m. $Z = 3 \times 10^{-4}$

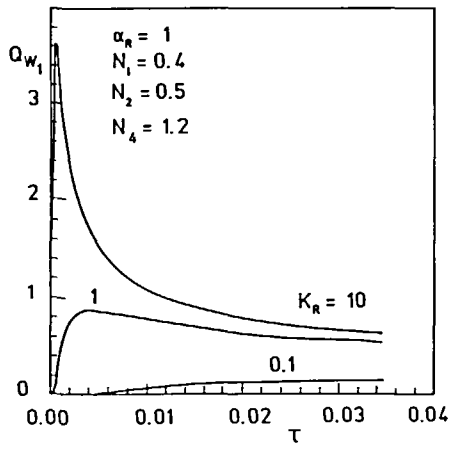

Figure 9 Effect of K_R on the transient behaviour of the inner wall heat flux, $Z = 12 \times 10^{-4}$

interfacial temperature, the mixing cup temperature and the inner wall interfacial heat flux, respectively. In each of these figures curves corresponding to three values of K_R are presented, namely, $K_R = 0.1$, 1 and 10. These figures clearly indicate that K_R has pronounced effects on unsteady heat transfer in laminar annular flows. For a given τ, increasing the value of K_R (i.e., increasing the thermal conductivity of the wall) causes an increase in the value of each of the three variables under consideration (θ_{w1}, θ_m, Q_{w1}), as shown in these figures. Also, at a given time, as the value of K_R increases the dimensionless temperature of the inner solid-fluid interface is closer to the new (step) value of the inner surface temperature of the inside tube ($\theta = 1$). Moreover, by increasing the value of K_R the interfacial temperature (θ_{w1}) approaches its steady-state value faster. This can be clearly seen in *Figure 7*, with $K_R = 10$, θ_{w1} reaches an almost isothermal situation after relatively short period of time (small value of τ). This is indeed due to the direct increase in the wall thermal diffusivity (α_s) as a result of the increase in its thermal conductivity. Consequently, the response of the wall to the thermal transient will be faster with high values of K_R.

The effects of the wall-to-fluid thermal diffusivity ratio (α_R) on the unsteady conjugate heat transfer variables θ_{w1} and Q_{w1} (for given values of Z in the same previously mentioned annulus) are given in *Figures 10* and *11*, respectively. In each figure, curves corresponding to two values of α_R are presented, namely, $\alpha_R = 0.1$ and 10. As can be seen from these two figures, for a given ($\tau > Z/U_{max}$), increasing α_R causes an increase in the interfacial wall heat flux besides a decrease in the inner interfacial temperature. These behaviours can be attributed as follows. A large value of α_R implicitly means a large value of the product of the fluid density by its specific heat ($\rho_f C_f$). If the time is large enough so that convection has already showed up, increasing the value of $\rho_f C_f$ would produce more cooling to the solid-fluid interface, hence a reduction in θ_{w1} and an increase in Q_{w1}. On the other hand, it should be noted that at very small values of τ, when the conduction mode dominates the heat transfer process and the convection has not showed up yet, the previous influences of α_R on θ_{w1} and Q_{w1} may be reversed as could be noted in *Figure 11*.

Finally, *Figure 12* shows the effect of the walls thicknesses on the inner interfacial heat flux. This figure is for an annulus of $N_2 = 0.5$, $K_R = 10$ and $\alpha_R = 1$. As might be expected, this figure shows that increasing the walls thicknesses (one or both of them) produces an increase in the total thermal resistance of the system and hence reduces the heat transfer from the hot wall to the flowing fluid.

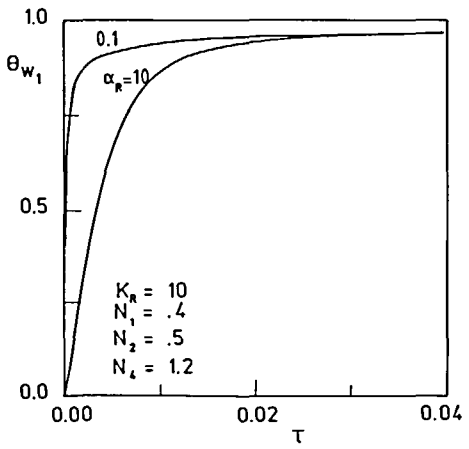

Figure 10 Effect of α_R on the transient behaviour of θ_{w1}, $Z = 3 \times 10^{-3}$

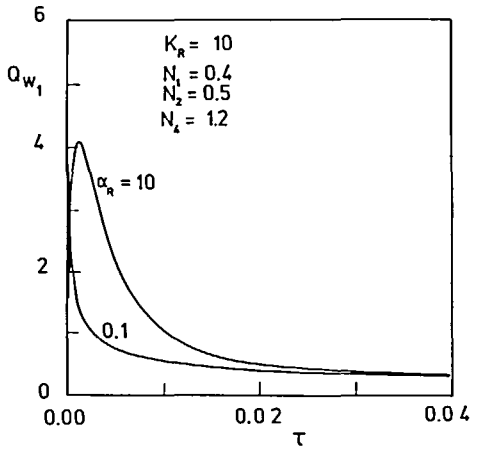

Figure 11 Effect of α_R on the transient behaviour of the inner wall heat flux, $Z = 3 \times 10^{-3}$

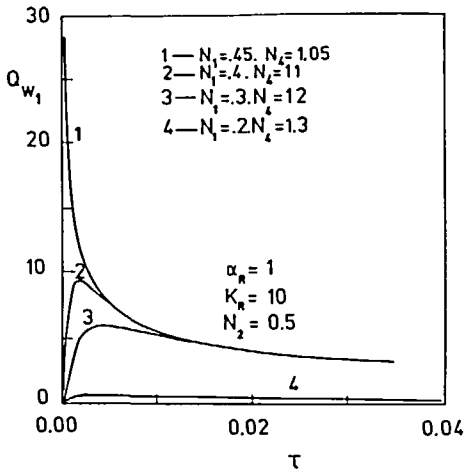

Figure 12 Effect of walls thicknesses on the inner wall heat flux

CONCLUSIONS

Transient conjugate heat transfer to laminar flows with constant physical properties and simultaneously developing hydrodynamic and thermal boundary layers in concentric annuli has been numerically studied. Thermal transient resulting from a step change in the inner surface temperature of the inside tube has been considered. The influences of the wall-to-fluid thermal conductivity ratio (K_R) and thermal diffusivity ratio (α_R) as well as the walls thicknesses have been investigated. From the presented results, it has been clearly seen that K_R, α_R and walls thicknesses have prominent effects on the transient heat transfer parameters. Therefore, it is not advisable to use the conventional assumption of extremely thin walls with infinite thermal conductivities and diffusivities particularly for systems with small values of K_R and α_R and very thick walls.

REFERENCES

1 Shah, R. K. and London, A. L. *Laminar Flow Forced Convection in Ducts*, Academic Press, New York (1978)
2 Mori, S., Inoue, T. and Tanimoto, A. Heat transfer to laminar flow with temperature-dependent heat generation, *The Canadian J. of Chemical Eng.*, **55**, 138–144 (1977)
3 Mori, S., Inoue, T. and Tanimoto, A. Heat transfer to laminar flow between parallel plates with interfacial heat generation, *J. Chemical Eng. Japan*, **11**, 83–88 (1978)
4 Mori, S., Kawamura, Y. and Tanimoto, A. Conjugated heat transfer to laminar flow with internal heat source in a parallel plate channel, *The Canadian J. of Chemical Eng.*, **57**, 698–703 (1979)
5 Faghri, M. and Sparrow, E. M. Simultaneous wall and fluid axial conduction in laminar pipe-flow heat transfer, *J. Heat Transfer*, **102**, 58–63 (1980)
6 Barozzi, G. S. and Pagliarini, G. A method to solve conjugate heat transfer problems: The case of fully developed laminar flow in a pipe, *J. Heat Transfer*, **107**, 77–83 (1985)
7 Pagliarini, G. Conjugate heat transfer for simultaneously developing laminar flow in a circular tube, *J. Heat Transfer*, **113**, 763–766 (1991)
8 Sakakibara, M., Mori, S. and Tanimoto, A. Conjugate heat transfer with laminar flow in an annulus, *The Canadian J. of Chemical Eng.*, **65**, 541–549 (1987)
9 Kirshan, B. On conjugated heat transfer in fully developed flow, *Int. J. Heat Mass Transfer*, **30**, 288–289 (1982)
10 Olek, S., Ellias, E., Wacholder, E. and Kaizerman, S. Unsteady conjugated heat transfer in laminar pipe flow, *Int. J. Heat Mass Transfer*, **34**, 1443–1450 (1991)
11 Cotta, R. M., Mikhailov, M. D. and Ozisik, M. N. Transient conjugated forced convection with periodically varying inlet temperature, *Int. J. Heat Mass Transfer*, **30**, 2073–2082 (1987)

12 Lin, T. F. and Kuo, J. C. Transient conjugated heat transfer in fully developed laminar pipe flows, *Int. J. Heat Mass Transfer*, **31**, 1093–1102 (1988)
13 Yan, W. M., Tsay, Y. L. and Lin, T. F. Transient conjugated heat transfer in laminar pipe flows, *Int. J. Heat Mass Transfer*, **32**, 775–777 (1989)
14 El-Shaarawi, M. A. I. Heat transfer and hydrodynamics in the entrance region of concentric annuli with stationary and rotating inner walls, *PhD Thesis*, The University of Leeds, Leeds, UK (1974)
15 Coney, J. E. R. and El-Shaarawi, M. A. I. Finite difference analysis for laminar flow heat transfer in concentric annuli with simultaneously developing hydrodynamic and thermal boundary layers, *Int. J. Numer. Methods Eng.*, **9**, 17–38 (1975)
16 El-Shaarawi, M. A. I. and Sarhan, A. Combined forced-free laminar convection in the entry region of a vertical annulus with a rotating inner cylinder, *Int. J. Heat Mass Transfer*, **25**, 175–186 (1982)
17 Bodoia, J. R. and Osterle, J. F. Finite difference analysis of plane Poiseuille and Couette flow developments, *Appl. Sci. Res.*, **A10**, 265–276 (1961)
18 Patankar, S. V. *Numerical Heat Transfer and Fluid Flow*, Hemisphere Publishing Corp. (1980)
19 Siegel, R. and Sparrow, E. M. Transient heat transfer from laminar forced convection in the thermal entrance region of flat ducts, *J. Heat Transfer*, **81**, 29–36 (1959)
20 Cotta, R. M. and Ozisik, M. N. Transient forced convection in laminar channel flow with time-wise variations of wall temperature, *ASME Paper 85-WA/HT-72* (1985)